Hindawi
International Journal of Polymer Science
Volume 2022, Article ID 3399986, 12 pages
https://doi.org/10.1155/2022/3399986

Research Article

Effect of the Addition of Oil Palm Mesocarp Fibers on the Physical and Mechanical Properties of a Polyester Matrix Composite

Paul William Mejouyo Huisken[1,2] **Gilbert Tchemou**[1,2] **Nicodème Rodrigue Sikame Tagne**[2] **Dieunedort Ndapeu**[2] **and Ebenezer Njeugna**[1,2]

[1]*Laboratory of Mechanics (LM), University of Douala, Douala, Cameroon*
[2]*Laboratory of Mechanics and Appropriate Materials (LAMMA), University of Douala, Douala, Cameroon*

Correspondence should be addressed to Paul William Mejouyo Huisken; huiskenwilliam@gmail.com

Received 29 November 2021; Revised 18 February 2022; Accepted 14 March 2022; Published 26 March 2022

Academic Editor: Yasir Nawab

This work focuses on the assessment of oil palm mesocarp fibers as reinforcement in a composite material with an unsaturated polyester matrix. Several volume ratios of OPMF reinforcement (0 to 15%) were used, the fibers being distributed randomly. The resulting composite was characterized on the physical and mechanical aspects. Physically, the true and apparent densities were determined as well as the porosity rate. It appears that the addition of fibers further lightens the composite and increases the porosity. The water absorption rate of the different composites samples was evaluated. The more fibers the composite contains, the higher its water absorption rate. On the mechanical aspect, the bending modulus of elasticity, bending stress at break, and breaking strain were evaluated through a three-point bending test on all combinations. The same parameters were also evaluated for certain combinations by a unidirectional tensile test. It appears from this mechanical characterization that the volume fraction of 5% reinforcement has the highest specific modulus. Impact tests were performed on samples of this combination using several sizes of reinforcing fibers. Impact resistance is enhanced as the size of the inclusion increases. The Halpin-Tsai micromechanical model for randomly distributed short fiber composites was used for the inverse approach determination of the theoretical moduli of the matrix and OPMF, then in a direct approach to determine the elastic modulus of the composite at 7.5% reinforcement.

1. Introduction

The use of plant fibers to replace synthetic fibers in the reinforcement of composite materials has really taken off in the last decade. In addition to being environmentally sustainable, these composites in some cases have technical and usage properties close to synthetic fiber composites [1]. If plant fibers are criticized for their great hydrophobicity, their great lightness and their mechanical properties acceptable for use in many fields can be recognize [2–5]. In addition, many treatments, although most of them are chemical, improve their resistance to water and humidity and promote their use [6–8]. The fields of use for plant fiber composites are varied. They are found in the automotive industry, sport, aeronautics, energy, furniture, construction, and many other fields [9]. These new construction materials made from recycled plastic waste, mining waste or plant fibers, represent one of the best ways to solve environmental challenges according to the logic of sustainable development [10–12]. They reduce greenhouse gas emissions, limit energy consumption, and optimize the use of nonrenewable natural resources. The use of agricultural residues therefore becomes a reliable alternative to solve current technical as well as environmental problems such as the depletion of primary resources, the improvement of certain technical properties by the use of conventional materials (density, rigidity, thermal conductivity, and dimensional stability), and pollution by agricultural and industrial by-products [11, 13].

The plant fibers used for these composites come from various origins (leaves, fruit, trunks, roots, etc.), and many plants are the subject of study. Jute, sisal, cotton, coconut, and ramie fibers are widely tested and used in the manufacture of biocomposites. The choice of fibers is often justified by their availability, their technical properties, and their compatibility with the matrix, which can be a thermosetting or thermoplastic polymer [1, 14]. In some cases, the fibers are woven to produce fabrics serving as reinforcement for the composites. The influence of weaving strategies is also discussed in the literature [15]. Some plant fibers, such as oil palm mesocarp fibers (OPMF), although abundantly available because of the industrial production of palm oil, are still poorly used for the reinforcement of biobased composites.

The main works in the literature on the particular use of OPMFs in the manufacture of composites are those of Okafor [16] in the reinforcement of a ceramic matrix for tiles production. The results show a considerable improvement in the wear properties of the tile; however, the resistance to humidity and water is strongly influenced. Epoxy resin is also reinforced by OPMF by Yussof et al. [17]. Results show improvement in modulus of elasticity for 5% volume reinforcement in OPMF, but continued decrease in flexural stress and elongation with fiber inclusion. Other resins such as polypropylene (PP), polyvinyl chloride (PVC), Phenol formaldehyde (PF), and polyurethane (PU) [18] are also reinforced with fibers from oil palm. These composites have acceptable physical and mechanical performances for their use in fields such as aerospace, automotive parts, sports and recreation equipment, boats, office products, machinery [19]. Whatever the biocomposite, the challenges lie in the choice of volume fractions, architecture, and sizes of particles or fibers to optimize the physical and mechanical performance [20–22].

This research work focuses on the effect of the rate of reinforcement in OPMF on the physical properties (density, porosity, and water absorption rate) [23], and mechanical (bending, tensile, and impact test) of a polyester matrix biocomposite. The experimental approach is discussed here. It is then coupled with a theoretical micromechanical approach based on the Halpin-Tsai composite homogenization theory on the mechanical properties of composites.

2. Materials and Methods

2.1. UP-OPMF Composite Formulation. Fibers from a palm oil production factory in the city of Nkongsamba-Cameroon are washed in a 5% sodium hydroxide (NaOH) solution. They are then dried for three days away from the sun. Seven (07) mixtures corresponding to different reinforcement volume rates are then formulated. They are referred to as UP-OPMF-X. X is the volume fraction of fiber in the mixture and UP-100 to the samples without fiber used as reference as shown in Table 1.

In practice, due to the difficulty of measuring fiber volume, the law of mixtures has been used to convert volume fractions (ϑ_f and ϑ_m) to mass fraction (m_f and m_m).

$$\begin{cases} m_f = \dfrac{\rho_f}{\rho_f.\vartheta_f + \rho_m\left(1-\vartheta_f\right)}\vartheta_f, \\ m_m = \dfrac{\rho_m}{\rho_f.\vartheta_f + \rho_m\left(1-\vartheta_f\right)}\vartheta_m, \end{cases} \tag{1}$$

where ϑ_f and ϑ_m, respectively, the volume fractions of the fiber and matrix, ρ_f and ρ_m their densities, $\rho_f = 1206\,\text{kg/m}^3$ [24], and $\rho_m = 1300\,\text{kg/m}^3$ [25].

Cold compression contact molding [26] was used for the manufacture of composites in the form of composite plates of dimension $10 \times 90 \times 150$ mm which will subsequently be machined to produce the specimens for the various tests.

2.2. Experimental Characterization of UP-OPMF Composite

2.2.1. Determining the Apparent Density of the Composite. Specimens used for the determination of the apparent density are of dimensions $7\,\text{mm} \times 15\,\text{mm} \times 30\,\text{mm}$ (Figure 1). For each combination, six specimens were used, and the average density of the combination is calculated.

The apparent density is calculated using

$$\rho_a = \frac{m}{V_{ac}}, \tag{2}$$

where ρ_a is the bulk density of the sample in kg/m^3, m is the mass of the sample in kg, and V_{ac} is the apparent volume of the composite in m^3 calculated from the dimensions of the specimen.

2.2.2. Determination of the True Density of the Composite. The specimens used for the determination of the true density of the composite have a geometry similar to those in Figure 1. The gravimetric method was used to evaluate the volume of a column of water displaced in a beaker. The sample is weighed before being immersed in water, and its mass is noted m. it is then immersed in water and causes a variation ΔV of the volume in the beaker. The true density is then determined by Equation (3). For each of the combinations, 06 specimens are used, and the average density of the combination is calculated.

$$\rho_r = \frac{m}{V_{rc}}, \tag{3}$$

where ρ_r is the true density of the sample in kg/m^3, m is the mass of the sample in kg, and V_{rc} is the volume of the composite in m^3 corresponding to the change in the volume of water.

2.2.3. Determination of the Porosity Ratio of the Composite. Depending on the manufacturing process, the porosity rate of composites is between 1 and 10%. A high porosity rate essentially results in significant drops in mechanical properties. A low level of porosity reflects a good compactness of the composites.

Table 1: Designation of the combinations according to the volume fraction of the fibers.

Samples	UP-100	UP-OPMF-2.5	UP-OPMF-5	UP-OPMF-7.5	UP-OPMF-10	UP-OPMF-12.5	UP-OPMF-15
Fiber volume fraction (%)	0	2.5	5	7.5	10	12.5	15

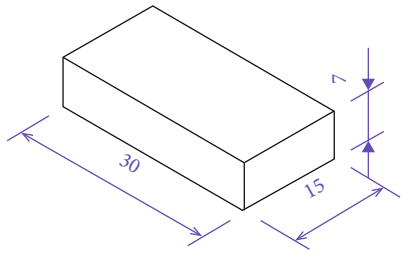

Figure 1: Specimen for determination of absorption rate and density.

Table 2: Definition of traditional Halpin-Tsai parameters for a composite reinforced with short fibers.

Designation	P	P_f	P_m	ζ
Longitudinal modulus	E_{11}	E_f	E_m	2 (l/d)
Transverse modulus	E_{22}	E_f	E_m	2
Longitudinal shear modulus	G_{12}	G_f	G_m	1

(l/d) represents the aspect ratio of the fiber.

The porosity $p(\%)$ of the UP-OPMF composite is calculated by Equation (4) [27].

$$p(\%) = \frac{(\rho_r - \rho_a)}{\rho_r} \times 100, \tag{4}$$

where ρ_r and ρ_a, respectively, are the true density and the apparent density in kg/m^3.

2.2.4. Determination of the Water Absorption Ratio of the UP-OPMF Composite. Specimens (Figure 1) are initially weighed and subsequently immersed in distilled water at room temperature. The gravimetric method is used. Initially, the test pieces are weighed every 5 min, and the new masses are noted. After observing that the mass does not vary considerably after 5 minutes, the duration of immersion in distilled water is increased to 10 minutes, 30 minutes, 60 min, and 120 min then every 1440 min. The operation is repeated until the mass no longer changes (saturation). At the time of the mass measurement, the samples are taken out of the bath and lightly wiped with an absorbent paper to remove the film of water present on the surface. The samples are then weighed and again immersed. A balance with an accuracy of 1 mg is used for these measurements, which are necessary for calculating the water absorption ratio using Equation (5) [28].

$$WR(\%) = \frac{W_s - W_0}{W_0} \times 100, \tag{5}$$

where W_0 is the initial mass of the sample and W_s is its mass at saturation.

2.2.5. Mechanical Characterization of the UP-OPMF Composite by the Three-Point Bending Test. The specimens used here are based on the BSI 2782 standard. They are of prismatic shape with a regular section of dimension $7 \times 15 \times 150$ mm [29]. Fifteen specimens for each of the 7 combinations were subjected to the 3-point static bending test until the material failed; the distance between supports L is 112 mm in accordance with the BSI 2782 standard. The force/displacement curve is plotted, and the static flexural modulus of elasticity E_{fl}, the flexural breaking stress σ_{Rf}, and the flexural breaking strain ε_{Rf} are calculated by Equations (6), (7), and (8), respectively, [22, 30].

$$\begin{aligned} \sigma_{Rf} &= \frac{3FL}{2lh^2}, \\ E_{fl} &= \frac{L^3}{4lh^3}\left(\frac{\Delta F}{\Delta f}\right), \\ \varepsilon_{Rf} &= \frac{6hf}{L^2}, \end{aligned} \tag{6}$$

where F is the force applied in (N), L is the distance between the supports in (mm), h and l are, respectively, the thickness and the width of the test piece in (mm), and f the deflection corresponding to the load F in (mm).

The ratio $(\Delta F/\Delta f)$ corresponds to the slope of the linear zone (elastic domain) of the force-displacement curve.

2.2.6. Mechanical Characterization of the UP-OPMF Composite by Unidirectional Tensile Test. The specimens of dimensions $7 \times 15 \times 150$ mm are used for the unidirectional tensile test. The BS EN ISO 527-5 [31] standard relating to the determination of the tensile properties of plastics/composites has been implemented. An average of five specimens per combination are tested. Only the combinations with 5, 7.5, and 10% volume ratio of reinforcement were studied. Relations (7), (8), and (9) are used for the calculation of the tensile stress σ_{Rt}, the tensile modulus of elasticity E_{tr}, and the ultimate strain of the composite ε_{Rt}.

$$\sigma_{Rt} = \frac{F_r}{hl}, \tag{7}$$

$$E_{tr} = \frac{\sigma}{\varepsilon}, \tag{8}$$

$$\varepsilon_{Rt} = \frac{L_u - L_0}{L_0}, \tag{9}$$

where Fr is the breaking force in (N), L_0 is the distance between the strain gauges in (mm) at the start of the test, h

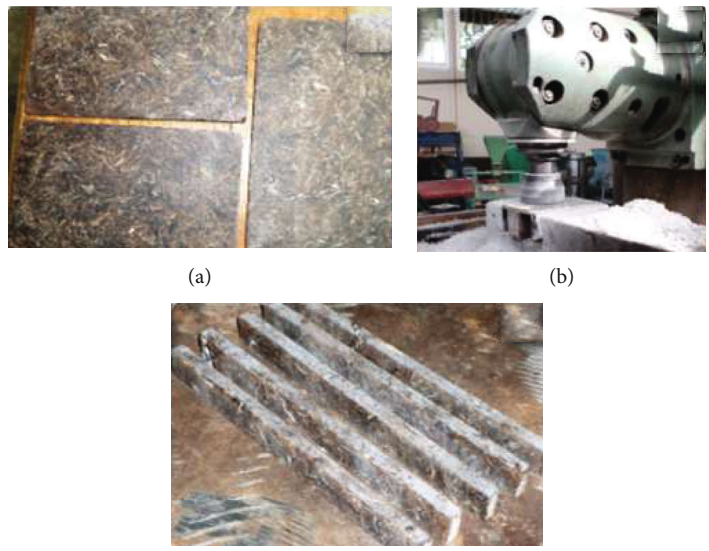

(a) (b)

(c)

Figure 2: UP-OPMF biocomposite obtained: (a) plates obtained by contact molding, (b) machining operation, (c) test beams obtained.

Table 3: Densities and porosity rate of the different samples.

Densities and porosity rate	UP-100	UP-OPMF-2.5	UP-OPMF-5	UP-OPMF-7.5	UP-OPMF-10	UP-OPMF-12.5	UP-OPMF-15
ρ_a (kg/m^3)	1192.5	1182.7	1176.6	1170.9	1165.4	1157.8	1153.1
SD	7.2	10.9	14.7	18.3	19.4	27.9	14.8
ρ_r (kg/m^3)	1219.6	1216.2	1214.2	1209.6	1203.1	1198.4	1194.4
SD	8.9	9.3	12.4	8.7	13.3	6.4	5.0
ρ_t (kg/m^3)	1219.6	1219.2	1218.9	1218.6	1218.2	1217.9	1217.5
Porosity rate	2.216	2.750	3.099	3.131	3.197	3.388	3.462
SD	0.81	0.85	0.84	0.48	0.69	0.23	0.34

ρ_a: apparent density; ρ_r: true density; ρ_t: theoretical density.

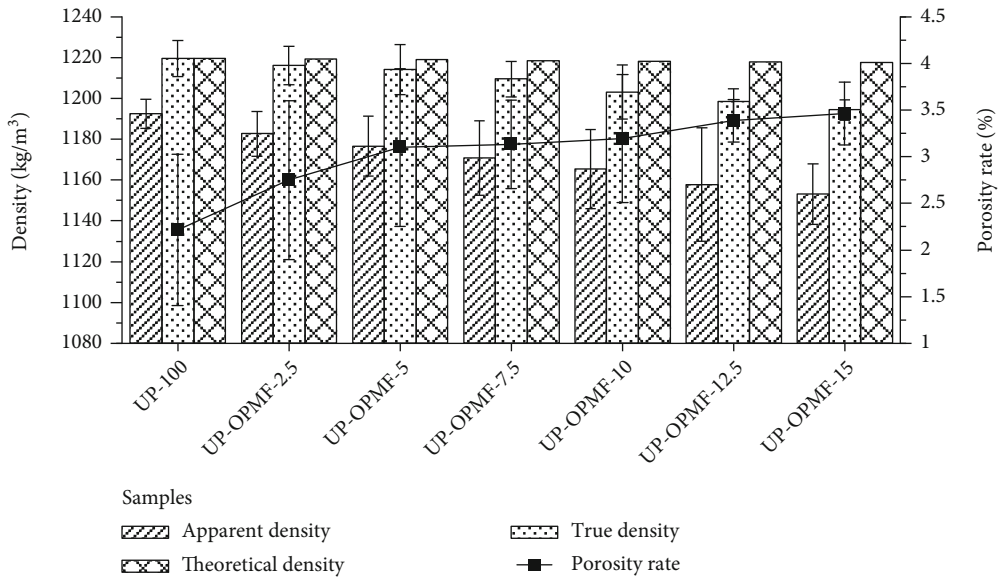

Figure 3: Density and porosity rate of the UP-OPMF composite.

Table 4: Summary results of the absorption rate of different e UP-OPMF composite combinations.

Samples	UP-OPMF-0	UP-OPMF-2.5	UP-OPMF-5	UP-OPMF-7.5	UP-OPMF-10	UP-OPMF-12.5	UP-OPMF-15
Absorption rate (%)	0.131	1.247	4.116	5.527	7.185	11.526	17.064
SD	0.03	0.05	0.60	0.50	0.62	1.23	2.38

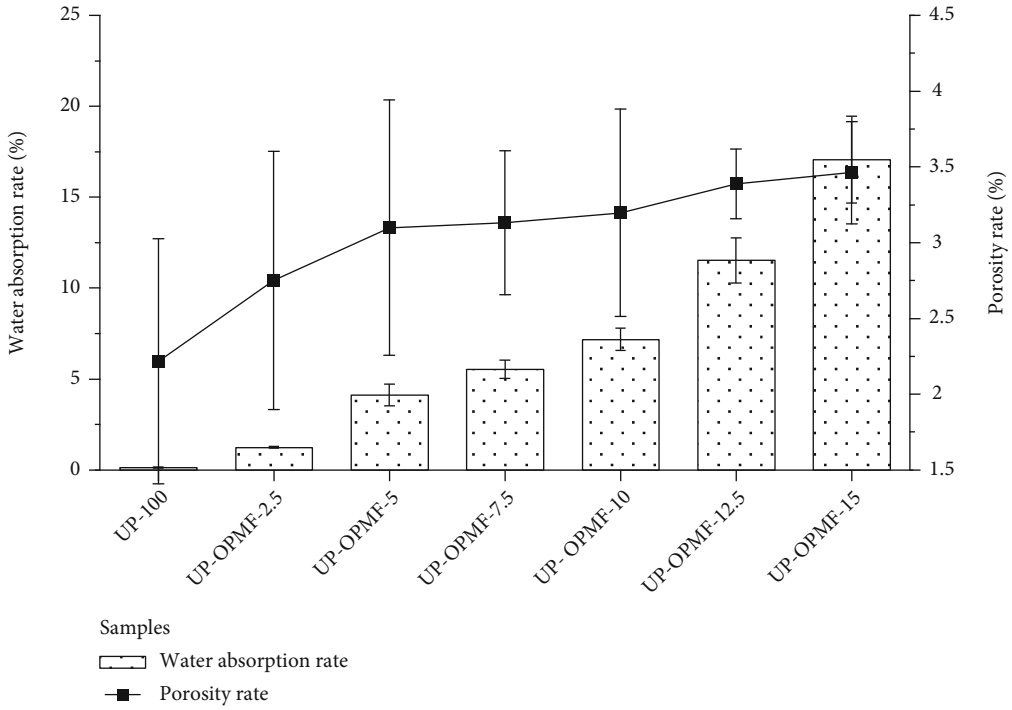

Figure 4: Distribution of the absorption rate of the different samples.

Table 5: Longitudinal three-point flexural modulus of different combinations of the UP-OPMF composite.

Samples	UP-100	UP-OPMF-2.5	UP-OPMF-5	UP-OPMF-7.5	UP-OPMF-10	UP-OPMF-12.5	UP-OPMF-15
E_{fl} (MPa)	2319.6	2346	2489	2013.3	1745	1504	1218.8
SD	127.0	184.3	257.3	169.4	98.5	205.0	161.0
σ_{Rt}(MPa)	61.7	23.3	27.0	28.6	28.6	23.3	22.6
ε_{Rt} (%)	2.81	0.94	1.10	1.64	1.97	1.98	2.28

and l are, respectively, the thickness and the width of the test piece in (mm), and L_u the length of the test specimen at break in (mm).

2.2.7. Determination of the Impact Strength of the Composite. Impact strength characterizes the material's ability to withstand shocks [32, 33]. The Charpy pendulum test [34] is performed here. This test is carried out in accordance with the ASTM D256 standard. Prismatic specimens of rectangular sections were used for this test [35]. Only the 5% combination of fiber reinforcement rate was investigated. The influence of the size of the reinforcing inclusions on the impact resistance of the composite was evaluated. For this purpose, the fibers were crushed and then sieved to obtain different sizes (0.5, 1.5, 2.5, 4, and 5 mm). 10 specimens per formulation were tested, and the average value of the impact strength was calculated.

During the test, the specimen is placed between two jaws, then the pendulum is moved from its equilibrium position by an angle θ_i, and released without initial speed. As it passes vertically, it strikes the specimen and breaks it, then rises at an angle θ_f. The energy absorbed by the specimen is obtained by subtracting from the energy stored at position θ_i that which remains after rupture of the specimen and allows the lift (residual energy). Equation (10) allows the calculation of the fracture energy W_a (J) and the impact strength K (J/m^2).

$$W_a = m_p g l\left(\cos\theta_i - \cos\theta_f\right),$$
$$K = \frac{W_a}{S}, \tag{10}$$

where m_p is the mass of the pendulum (100 g), g the

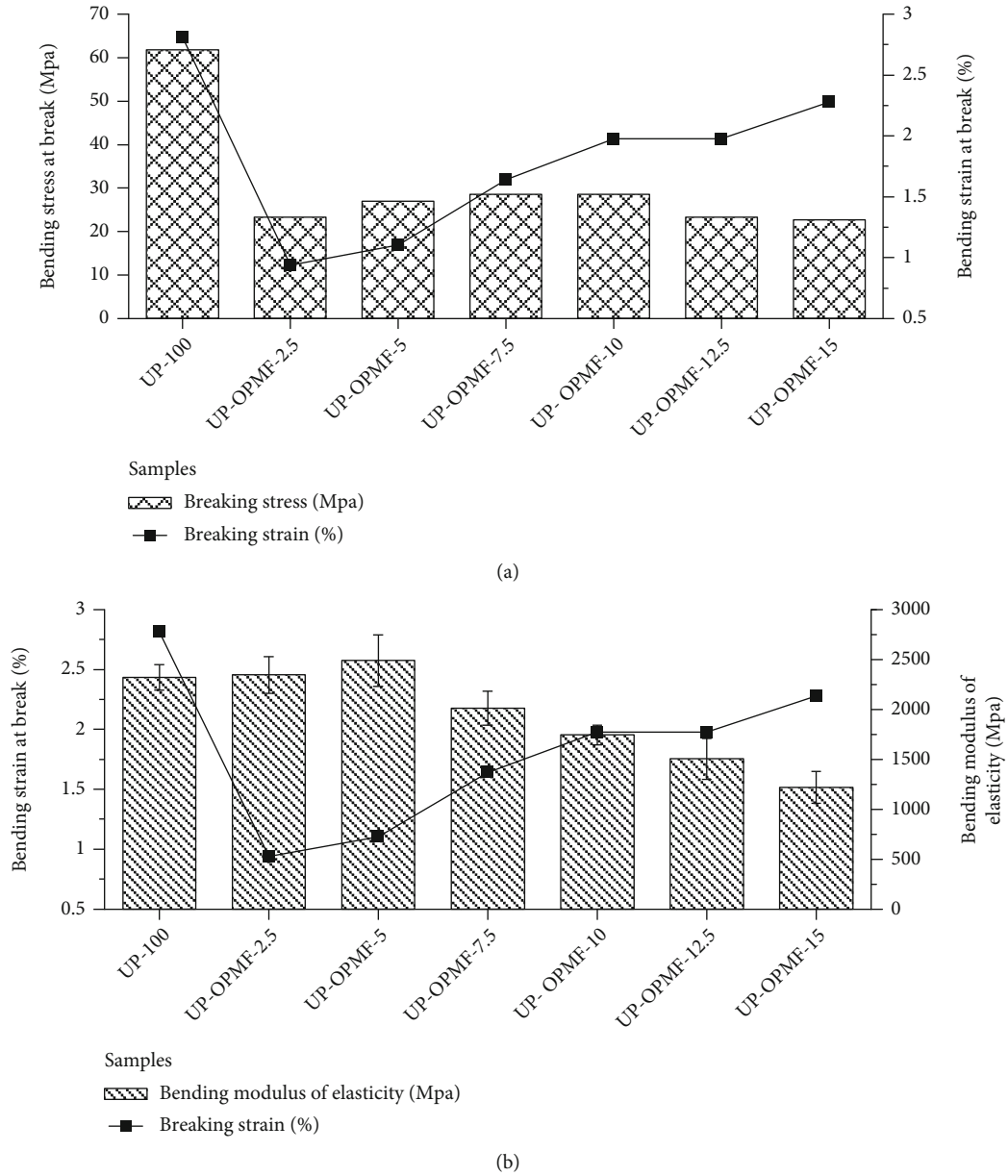

Figure 5: Distribution of the bending parameters of the UP-OPMF composite: (a) bending stress at break-bending strain at break, (b) bending strain at break-bending modulus of elasticity.

Table 6: Longitudinal tensile modulus of elasticity of the different combinations of the UP-OPMF composite.

Samples	UP-OPMF-5	UP-OPMF-7.5	UP-OPMF-10
E_{tr} (MPa)	3318.5	3058	2930.3
σ_{Rt} (MPa)	11.30	5.96	8.30
ε_{Rt} (%)	1.14	0.54	0.73

acceleration of gravity (10 N/kg), l is the length of the pendulum arm (130 mm), and S the section of the specimen.

2.3. Halpin-Tsai Model Applied to the UP-OPMF Composite. The theoretical modulus of elasticity of the composite was determined using micromechanical homogenization techniques [36, 37] valid for the short-fiber composites randomly dispersed from Halpin-Tsai. The Halpin-Tsai model uses the mechanical properties of the fiber and the matrix to calculate the mechanical properties of the randomly dispersed fiber composite. The objective is to obtain results that can serve as a basis for discussion on the molding protocol, to speculate on the structural defects that may result from this forming technique as well as the compatibility between the polyester matrix and the OPMF. Equations (11) and (12) present this formulation [16].

$$\frac{P}{P_m} = \frac{1 + \zeta \eta v_f}{1 - \eta v_f}, \tag{11}$$

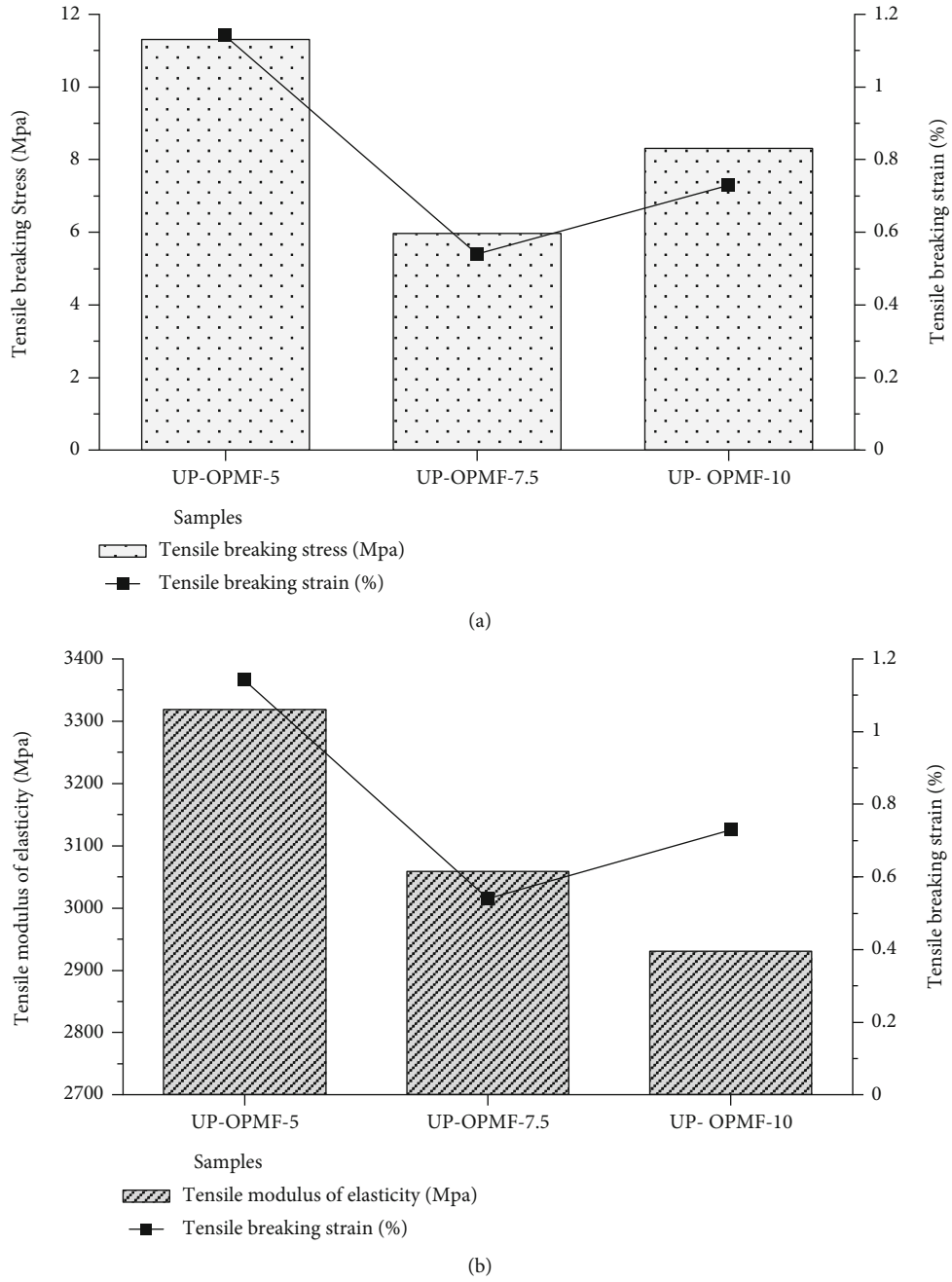

Figure 6: Distribution of tensile properties of the UP-OPMF composite: (a) tensile stress at break-tensile strain at break; (b) tensile modulus of elasticity-tensile strain at break.

where

$$\eta = \frac{\left(P_f/P_m\right) - 1}{\left(P_f/P_m\right) + \zeta}. \tag{12}$$

P, P_f, and P_m are the respective moduli (longitudinal, transverse, or shear) of the composite, the fiber, and the matrix. ζ is a constant defining the aspect ratio of the fiber. These parameters are detailed in Table 2.

The Halpin-Tsai model was used in the case of this work in reverse approach. For this purpose, the longitudinal modulus of elasticity obtained in unidirectional traction (E_{tr}) of two combinations of the composite (5 and 10%) is used to determine the theoretical modulus of elasticity of the matrix (E_{mth}) and of the fiber (E_{fth}). These theoretical moduli are reused in the direct homogenization approach to predict the theoretical modulus of elasticity of the sample at 7.5% and compare it to those obtained experimentally in unidirectional tension and in three-point bending. This approach is implemented by a system of two equations

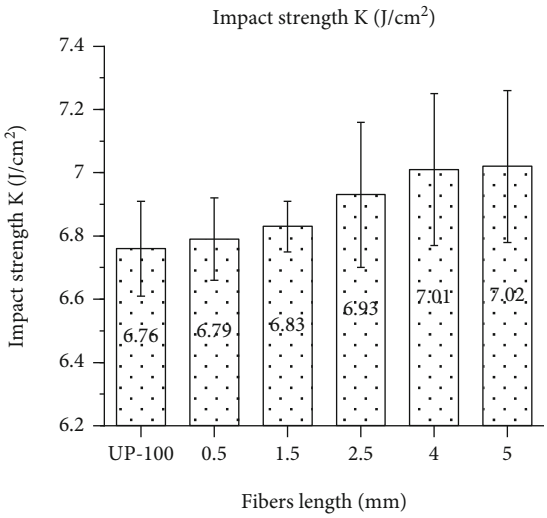

Figure 7: Impact strength distribution of UP/OPMF composite as a function of fiber size.

summarized by 15.

$$\eta\xi\vartheta_{fi}E_m + \eta\vartheta_{fi}E_{ci} = E_{ci} - E_m, \quad (13)$$

where $\vartheta_{fi} \in \langle 5\,;10\rangle$ is the volume ratio of composite i and E_{ci} is the unidirectional tensile modulus of elasticity of the composite having the volume fraction ϑ_{fi}.

3. Results and Discussions

3.1. Composite UP-OPMF. At the end of the contact molding, the composite obtained has a light brown appearance indicative of the presence of the OPMFs. It is rigid and easily machinable, and the fibers are dispersed randomly but uniformly. The plates of Figure 2(a) have in fact been sawn on an edger and then surfaced with a milling machine (Figure 2(b)) to obtain the beam specimens of Figure 2(c).

The parts likely to undergo conventional machining (drilling, sawing, surfacing, etc.) can, if the usage properties allow it, be molded and then machined in UP-OPMF biocomposite.

3.2. Physical Characteristics of the UP-OPMF Composite

3.2.1. Apparent, True, Theoretical Densities and Porosity Rate of the UP-OPMF Composite. The apparent and true densities obtained experimentally are presented in Table 3. There is also the theoretical density obtained by calculation of homogenization from the densities of the constituents as well as the porosity rate of the various samples.

Table 3 highlights the difference between true densities and theoretical densities significant for the existence of porosities within the material. The variations of the different densities and the rate of porosity with the ratio of volume of reinforcement in fibers can be appreciated in Figure 3.

All densities decrease as the percentage of fiber increases. This result is in agreement with the specific literature on composites. However, the variation is more pronounced on the experimental values compared to those obtained by the homogenization theories. This calls into questioning the validity of theoretical homogenization models. A comparison of the true and theoretical densities of the composite makes it possible to demonstrate the porous nature of the material. It is observed that the presence of the fibers increases the level of porosity of the material. These porosity values are however lower than those obtained for other composites in the literature [38, 39] and are well below the maximum permissible porosity threshold for large diffusion (GD) composites which is approximately 10% [22].

3.2.2. Water Absorption Rate in the UP-OPMF Composite. Saturation is observed for all samples after the fourth hour of immersion. The average absorption rates as well as the standard deviations are presented in Table 4.

Table 4 highlights the fact that adding fibers to the composite increases its water absorption capacity and may affect its durability. Figure 4 shows the evolution of the absorption rate as a function of the reinforcement ratio.

The water absorption rate of UP-OPMF composites is correlated with the porosity rate although the trend of the curves is not exactly the same. The increasing of the absorption can be linked to hydrophilicity character of lignocellulosic fibers. By including 15% of OPMF in the matrix, there is an approximately 17% increase in water absorption (Figure 4). This suggests the need to consider treatments to reduce the hydrophilicity of OPMFs prior to their insertion into such composites. However, this absorption edge is acceptable for the materials of the front building industry serve interior trim, ceiling, or partition walls. Moreover, these composites can undergo the surface treatments (coating, varnish) commonly applied to wood to reduce their absorbent character.

3.3. Mechanical Bending Properties of the UP-OPMF Composite. The variation of the mechanical bending properties of the UP-OPMF composite is presented in Table 5.

From this table, it can be said that the addition of OPMF affects the mechanical flexural properties of polyester. The evolution of the flexural strength of the composite, the breaking strain, and the flexural modulus of elasticity as a function of the reinforcement rate is presented in Figure 5.

The addition of OPMFs in the polyester matrix reduces the flexural breaking stress as well as the flexural breaking strain by almost 60%. This reduction is certainly due to the presence of reinforcing fiber which generates areas of stress concentration, the low adhesion at the interface, and the inherent mechanical properties of the fibers which are weaker than those of the matrix. Since these fibers are low in number, there is a low charge transfer capacity and therefore a low level of resistance of the composite. This level of resistance improves with the increase in the number of fibers and therefore the charge transfer capacity; this results in an increase in the bending breaking stress between 2.5 and 10% of fiber reinforcement. A similar result was also obtained in the literature [40] for the hybrid composite PLA/PCL/nanoclay/OPMF. Beyond this reinforcement

Table 7: Comparison of the impact strength of the different composites reinforced with vegetable fibers.

Composites	K (J/cm^2)	Year	References
Epoxy/Kénaf-Kevlar	3.8–17.9	2016	[32]
Epoxy/bamboo	37.5		
Epoxy/bamboo-banana	62.5	2016	[34]
Epoxy/bamboo-linen	50		
Polyester/sisal-banana-PALF	16		
Polyester/sisal-PALF	6		
Polyester/banana-PALF	4	2014	[43]
Polyester/sisal-GFRP	2		
Polyester/banana-GFRP	1		
Poly(L-lactic acid)/jute	1.29	2016	[44]
Polyester/Curaua	3.35	2014	[45]
Epoxy/lin	11–12.4	2016	[46]
Poly (butylene succinate) PBS/OPMF	0.5-4.2	2013	[35]
Poly (butylene succinate) PBS/OPMF	6.57	2014	[47]
PBS/(superheated steam) SHSOPMF	7.4		
PLA/PCL/nanoclay-OPMF	9.54-14.16	2014	[41]
Polyester/OPMF	**6.79–7.02**	**Case studied**	

Table 8: Theoretical moduli of elasticity of the fiber and of the matrix by the inverse Halpin-Tsai approach.

ν_f (%)	E_{tr} (MPa)	E_{mth} (MPa)	E_{fth} (MPa)
5	3318.54	3459.37	3431.19
10	2930.30		

Table 9: Comparison between theoretical and true moduli of elasticity of the matrix and the fiber.

	Matrix (polyester)	Fiber (OPMF)
Theoretical modulus of elasticity (MPa)	3459.37	3431.19
Experimental modulus of elasticity (MPa)	2319.60*	3273.35**
Relative error (%)	32.95	4.60

*Experimental modulus of elasticity of the matrix obtained by three-point bending test. **Average modulus of elasticity of OPMF of the Pissifera variety [48].

Table 10: Theoretical moduli of elasticity of the composite at 7.5% fibers by Halpin-Tsai direct approach.

ν_f (%)	E_{tr} (MPa)	E_{th} (MPa)	Relative error (%)
7.5	3058.00	3247.8	5.8

value, although the elongation capacity of the material before rupture continues to increase, the bending breaking stress drops, indicating that the reinforcement limit threshold has been reached.

The longitudinal modulus of elasticity increases up to 5% reinforcement. Beyond this value, it drops continuously with increasing fiber content. In view of the bending results, the composite with 5% reinforcement seems to present the best compromise between the different properties.

3.4. Tensile Mechanical Properties of UP-OPMF Composite. Unidirectional tensile tests were performed on specimens of the 5, 7.5, and 10% combinations. For each of these combinations, the longitudinal modulus of elasticity, the breaking stress as well as the tensile breaking strain is determined. Table 6 summarizes the different parameters obtained for each of the combinations tested.

In view of the tensile results, it is observed that the modulus of elasticity of the UP-OPMF-5 composite is higher than that of the other combinations. In addition, its tensile strength at break as well as its breaking strain is the highest. A similar behavior is also described in the literature by Zuhri et al. [17]. Figure 6 shows the distribution of the different tensile properties as a function of the reinforcement ratio.

The breaking strength and the breaking strain evolve in a similar way. An unexplained drop is observed for the 7.5% fiber combination. The modulus of elasticity decreases with the addition of fibers. While the magnitude is the same for the tensile modulus of elasticity with those of the three-point bending test, we can see that it is higher in the tensile case. This would come from the fact that the fibers, although distributed randomly, have a particular distribution plane resulting in a plane orthotropy of the composite. Similar behavior was reported by Eng et al. [41] in the case of reinforcement of hybrid composites PLA/PCL/nanoclay/OPMF.

3.5. Impact Behavior of the UP-OPMF Composite. Due to the fact that the 5% composite presented the best mechanical properties, only specimens reinforced with 5% fibers of different sizes (0.5, 1.5, 2.5, 4, and 5) were tested as well as an unreinforced control specimen. It is observed on the one

Table 11: Specific moduli of the different combinations of the UP-OPMF composite.

Specific moduli	UP-OPMF-0	UP-OPMF-2.5	UP-OPMF-5	UP-OPMF-7.5	UP-OPMF-10	UP-OPMF-12.5	UP-OPMF-15
E_{fe}/ρ_r	1.9	1.93	2.05	1.66	1.45	1.26	1.02
E_{tr}/ρ_r			2.62	2.41	2.31		

hand an increase in impact strength by the addition of OPMF fibers and on the other hand by an effect of the size of the reinforcing particles on the impact strength of the composite. Figure 7 shows this variation.

Although the rate of change appears to be low, impact strength increases with the size of the fibers. It can therefore be said that the higher the aspect ratio of the fibers, the more energy the composite absorbs before breaking. This would be due to the greater attachment surface of the fibers in the matrix preventing their loosening. A similar result is also described in the literature for a polyester/banana fiber composite [42]. A comparison of the impact strength values with other composites is given in Table 7.

The impact strength values of the UP-OPMF composite are much higher than those obtained for poly (L-lactic acid)/jute composites as well as all polyester matrix composites except the polyester/sisal-banana-PALF hybrid composite. However, they remain low compared to the values obtained for the various epoxy matrix composites.

3.6. Theoretical Modulus of Elasticity of the UP-OPMF Composite by Halpin-Tsai Theory. Applying the Halpin-Tsai homogenization theory, the theoretical moduli of elasticity of the fiber (E_{fth}) and matrix (E_{mth}) were determined by an inverse approach. For this, the tensile results of UP-OPMF composites with 5 and 10% fiber reinforcement were used as baseline data. Table 8 shows the results obtained.

Obviously, although being of the same order of magnitude, it is observed that the theoretical modulus of elasticity of the matrix is greater than that of the composite. A comparison between the theoretical and actual moduli of elasticities of the fiber and the matrix is made in Table 9.

There is a significant difference between the theoretical and experimental moduli of elasticity of the matrix. This difference would be due on the one hand to the fact that the modulus of elasticity in bending is underestimated compared to that in tension and on the other hand to the possible defects which would exist in the structure of the molded composite (porosities, foreign inclusions, and interface faults). For against, the theoretical modulus of the fiber is 4.6% almost identical to that obtained experimentally.

By direct homogenization approach, theoretical fiber and matrix values was used to determine the theoretical modulus of elasticity of the composite at 7.5% fiber reinforcement rate. Table 10 presents the results as well as the error made in the prediction process.

The theoretical modulus of elasticity is in the same order of magnitude (within 5.8%) as the experimental modulus of elasticity. The Halpin-Tsai homogenization technique therefore makes it possible to effectively predict the tensile modulus of elasticity of the UP-OPMF composite.

3.7. Specific Modulus of the UP-OPMF Composite. The specific tensile and flexural moduli of the composite were calculated. They are summarized in Table 11.

The 5% fiber-reinforced UP-OPMF composite has the highest specific modulus. It therefore has the best strength-to-weight ratio.

4. Conclusion

This work focused on the formulation, manufacture, and characterization of several combinations of an UP-OPMF composite with differential volume fractions of OPMF reinforcement and having as matrix the polyester resin. The different combinations of this composite have undergone physical characterization tests (density, porosity, and water absorption) and mechanical (flexion, traction, and impact strength). It appears that the density increases with the rate of fiber reinforcement. In addition, the true density is higher than the bulk density. This is due to the presence of the pores in the material. The porosity rate was therefore determined; it varies from 2.22 to 3.46%. Obviously, the more porous the material, the more absorbent it is. The average absorption rate ranges from 0.13 to 17%. Then, by a three-point bending test, the flexural modulus of elasticity of the UP-OPMF composite was determined. The modulus of elasticity obtained in three-point bending varies from 1218 to 2489 MPa with a peak for the reinforcement at 5%. The tensile modulus of elasticity, the breaking stress, and the breaking strain for the composites at 5, 7.5, and 10% was determined. As in the case of bending, the 5% composite is the one with the highest tensile modulus of elasticity (3318 MPa) as well as the stress and strain at break. By applying the Halpin-Tsai homogenization theory, the theoretical prediction of Young's modulus was made. It appears that the composite with 5% volume reinforcement is the one with the best specific modulus. Although some analyses are necessary to clarify the final use of the composite (analysis of the thermal behavior for example), the current results allow to conclude that this composite can be used in the building industry for the interior lining, the ceiling, or the partition walls.

Data Availability

The data used to support the findings of this study are available from the corresponding author upon request.

Conflicts of Interest

The authors declare that they have no known competing financial interests or personal relationships that could have appeared to influence the work reported in this paper.

Authors' Contributions

P.W.H.M., G.T., and N.R.S.T. are responsible for the conceptualization; P.W.H.M., N.R.S.T., and D.N. for the methodology; P.W.H.M. for the software; G.T. and E.N. for the supervision; P.W.H.M., G.T., and D.N. for the visualization; P.W.H.M., G.T., N.R.S.T., and D.N. for the writing—original draft; and P.W.H.M., G.T., N.R.S.T., and D.N. for the writing—review and editing. All authors have read and agreed to the published version of the manuscript.

Acknowledgments

The authors thank the Laboratoire de Physique et Mécanique Textile (LPMT), ENSISA-University of Haute Alsace, France, for their help on the tensile tests with the tensile machine (MTS 20/M) in this research.

References

[1] H. Awais, Y. Nawab, A. Amjad, A. Anjang, H. Md Akil, and M. S. Zainol Abidin, "Environmental benign natural fibre reinforced thermoplastic composites: a review," *Composites Part C: Open Access*, vol. 4, article 100082, 2021.

[2] M. Syduzzaman, M. A. Al Faruque, K. Bilisik, and M. Naebe, "Plant-based natural fibre reinforced composites: a review on fabrication, properties and applications," *Coatings*, vol. 10, no. 10, article 973, 2020.

[3] Z. Alemayehu, R. B. Nallamothu, M. Liben, S. K. Nallamothu, and A. K. Nallamothu, "Experimental investigation on characteristics of sisal fiber as composite material for light vehicle body applications," *Materials Today: Proceedings*, vol. 38, pp. 2439–2444, 2020.

[4] H. T. Sreenivas, N. Krishnamurthy, and G. R. Arpitha, "A comprehensive review on light weight kenaf fiber for automobiles," *International Journal of Lightweight Materials and Manufacture*, vol. 3, no. 4, pp. 328–337, 2020.

[5] S. Uz Zaman, S. Shahid, K. Shaker et al., "Development and characterization of chemical and fire resistant jute/unsaturated polyester composites," *Journal of the Textile Institute*, vol. 113, no. 3, pp. 484–493, 2022.

[6] P. F. Alao, L. Marrot, H. Kallakas, A. Just, T. Poltimäe, and J. Kers, "Effect of hemp fiber surface treatment on the moisture/water resistance and reaction to fire of reinforced pla composites," *Materials*, vol. 14, no. 15, pp. 1–17, 2021.

[7] A. M. M. Edeerozey, H. M. Akil, A. B. Azhar, and M. I. Z. Ariffin, "Chemical modification of kenaf fibers," *Materials Letters*, vol. 61, no. 10, pp. 2023–2025, 2007.

[8] D. Matykiewicz, M. Barczewski, O. Mysiukiewicz, and K. Skórczewska, "Comparison of various chemical treatments efficiency in relation to the properties of flax, hemp fibers and cotton trichomes," *Journal of Natural Fibers*, vol. 18, no. 5, pp. 735–751, 2021.

[9] L. Kerni, S. Singh, A. Patnaik, and N. Kumar, "A review on natural fiber reinforced composites," *Materials Today: Proceedings*, vol. 28, pp. 1616–1621, 2020.

[10] M. I. Khan, M. Umair, K. Shaker, A. Basit, Y. Nawab, and M. Kashif, "Impact of waste fibers on the mechanical performance of concrete composites," *Journal of the Textile Institute*, vol. 111, no. 11, pp. 1632–1640, 2020.

[11] A. Achour, F. Ghomari, and N. Belayachi, "Properties of cementitious mortars reinforced with natural fibers," *Journal of Adhesion Science and Technology*, vol. 31, no. 17, pp. 1938–1962, 2017.

[12] M. Boumhaout, L. Boukhattem, H. Hamdi, B. Benhamou, and F. Ait Nouh, "Thermomechanical characterization of a biocomposite building material: mortar reinforced with date palm fibers mesh," *Construction and Building Materials*, vol. 135, pp. 241–250, 2017.

[13] K. Shaker, R. M. W. U. Khan, M. Jabbar et al., "Extraction and characterization of novel fibers from Vernonia elaeagnifolia as a potential textile fiber," *Industrial Crops and Products*, vol. 152, article 112518, 2020.

[14] A. K. Sinha, H. K. Narang, and S. Bhattacharya, "Mechanical properties of hybrid polymer composites: a review," *Journal of the Brazilian Society of Mechanical Sciences and Engineering*, vol. 42, no. 8, 2020.

[15] Z. Abbas, S. Shahid, Y. Nawab, K. Shaker, and M. Umair, "Effect of glass microspheres and fabric weave structure on mechanical performance of hemp/green epoxy composites," *Polymer Composites*, vol. 41, no. 11, pp. 4771–4787, 2020.

[16] F. O. Okafor, *Span Optimization for Palmnut Fibre-Reinforced Mortar Roofing Tiles*, University of Abudja, Nigeria, 1994.

[17] M. Yusoff, M. S. Salit, N. Ismail, and R. Wirawan, "Mechanical properties of short random oil palm fibre reinforced epoxy composites," *Sains Malaysiana*, vol. 39, no. 1, pp. 87–92, 2010.

[18] S. Shinoj, R. Visvanathan, S. Panigrahi, and M. Kochubabu, "Oil palm fiber (OPF) and its composites: a review," *Industrial Crops and Products*, vol. 33, no. 1, pp. 7–22, 2011.

[19] O. Faruk, A. K. Bledzki, H. P. Fink, and M. Sain, "Biocomposites reinforced with natural fibers: 2000-2010," *Progress in Polymer Science*, vol. 37, no. 11, pp. 1552–1596, 2012.

[20] M. Baskaran, R. Hashim, N. Said et al., "Properties of binderless particleboard from oil palm trunk with addition of polyhydroxyalkanoates," *Composites. Part B, Engineering*, vol. 43, no. 3, pp. 1109–1116, 2012.

[21] R. Hashim, N. Saari, O. Sulaiman et al., "Effect of particle geometry on the properties of binderless particleboard manufactured from oil palm trunk," *Materials and Design*, vol. 31, no. 9, pp. 4251–4257, 2010.

[22] M. E. H. Bourahli, "Caractérisation d'un composite verre/époxy," 2014.

[23] A. Bergeret and P. Krawczak, "Liaison renfort/matrice comportement des composites," *Tech. l'ingénieur*, vol. 33, 19 pages, 2014.

[24] M. S. Sreekala, M. G. Kumaran, and S. Thomas, "Stress relaxation behaviour in oil palm fibres," *Materials Letters*, vol. 50, no. 4, pp. 263–273, 2001.

[25] P. H. Sankar, Y. V. M. Reddy, and K. H. Reddy, "The effect of fiber length on tensile properties of polyester resin composites reinforced by the fibers of Sansevieria trifasciata," *International Letters of Natural Sciences*, vol. 8, pp. 7–13, 2014.

[26] D. Gay, *Matériaux composites*, 2015.

[27] M. Le Troedec, *Caractérisation des interactions physico-chimiques dans un matériau composite à base de phyllosilicates, de chaux et de fibres cellulosiques*, Doctoral Dissertation, Limoges, 2009.

[28] D. Scida, M. Assarar, R. Ayad, and C. Poilâne, "Effet de l'humidité sur le comportement mécanique des composites à fibres de lin," 2011.

[29] 2014, //http://www.atomer.fr/1Dimensions-eprouvettes-essais-de-flexion.

[30] D. Croccolo, M. De Agostinis, S. Fini et al., "Mechanical characteristics of two environmentally friendly resins reinforced with flax fibers," *Strojniški vestnik-Journal of Mechanical Engineering*, vol. 61, no. 4, pp. 227–236, 2015.

[31] "Plastics-determination of tensile properties; part 5: test conditions for unidirectional fibre reinforced plastic composites," 2009.

[32] R. Yahaya, S. M. Sapuan, M. Jawaid, Z. Leman, and E. S. Zainudin, "Water absorption behaviour and impact strength of Kenaf-Kevlar reinforced epoxy hybrid composites," *Advanced Composites Letters*, vol. 25, no. 4, article 096369351602500403, 2016.

[33] J. M. Duell, "Impact testing of advanced composites," *Composites*, vol. 97, pp. 97–112, 2004.

[34] M. Ramachandran, S. Bansal, and P. Raichurkar, "Experimental study of bamboo using banana and linen fibre reinforced polymeric composites," *Perspectives on Science*, vol. 8, pp. 313–316, 2016.

[35] Y. Y. Then, N. A. Ibrahim, N. Zainuddin, H. Ariffin, and W. M. Z. Wan Yunus, "Oil palm mesocarp fiber as new lignocellulosic material for fabrication of polymer/fiber biocomposites," *International Journal of Polymer Science*, vol. 2013, 7 pages, 2013.

[36] D. H. Hoang, *Contribution à l 'homogeneisation de materiaux heterogenes viscoelastiques: Milieux aleatoires et périodiques et prise en compte des interfaces*, Université Paris-Est Marne la Valléee, France, 2012.

[37] J. E. Arbaoui, *Étude Comparative et Caractérisations Mécaniques des Structure Sandwichs Multicouches*, Université Paul Verlaine–METZ, Verlaine, 2009.

[38] B. E. Fabien, *Etude des propriétés thermomécaniques du plâtre renforcé de fibres végétales tropicales*, Université de Douala, Douala, 2012.

[39] C. de Kergariou, A. Le Duigou, V. Popineau et al., "Measure of porosity in flax fibres reinforced polylactic acid biocomposites," *Composites. Part A, Applied Science and Manufacturing*, vol. 141, article 106183, 2021.

[40] C. C. Eng, N. A. Ibrahim, N. Zainuddin, H. Ariffin, W. M. Z. W. Yunus, and Y. Y. Then, "Enhancement of mechanical and dynamic mechanical properties of hydrophilic nanoclay reinforced polylactic acid/polycaprolactone/oil palm mesocarp fiber hybrid composites," *International Journal of Polymer Science*, vol. 2014, 8 pages, 2014.

[41] C. C. Eng, N. A. Ibrahim, N. Zainuddin, H. Ariffin, and W. M. Z. W. Yunus, "Impact strength and flexural properties enhancement of methacrylate silane treated oil palm mesocarp fiber reinforced biodegradable hybrid composites," *Scientific World Journal*, vol. 2014, pp. 1–8, 2014.

[42] L. A. Pothan, S. Thomas, and N. R. Neelakantan, "Short banana fiber reinforced polyester composites: mechanical, failure and aging characteristics," *Journal of Reinforced Plastics and Composites*, vol. 16, no. 8, pp. 744–765, 1997.

[43] S. Rathika, K. Palanikumar, and P. S. Raghavan, "Physical performance of sisal-PALF-banana/glass fiber reinforced polyester hybrid composites," *Asian Journal of Chemistry*, vol. 26, no. 14, pp. 4157–4161, 2014.

[44] G. M. A. Khan, M. Terano, M. A. Gafur, and M. S. Alam, "Studies on the mechanical properties of woven jute fabric reinforced poly(l-lactic acid) composites," *Journal of King Saud University-Engineering Sciences*, vol. 28, no. 1, pp. 69–74, 2016.

[45] M. A. Barcelos, N. T. Simonassi, S. N. Monteiro, and F. M. Margem, "Impact strength of natural fibre composites measured by different test methods: a review," *MATEC Web of Conferences*, vol. 109, pp. 3580–3588, 2014.

[46] W. Wang, N. Chouw, and K. Jayaraman, "Effect of thickness on the impact resistance of flax fibre-reinforced polymer," *Journal of Reinforced Plastics and Composites*, vol. 35, no. 17, pp. 1277–1289, 2016.

[47] Y. Y. Then, N. A. Ibrahim, N. Zainuddin, H. Ariffin, W. M. Yunus, and B. W. Chieng, "The influence of green surface modification of oil palm mesocarp fiber by superheated steam on the mechanical properties and dimensional stability of oil palm mesocarp fiber/poly (butylene succinate) biocomposite," *International Journal of Molecular Sciences*, vol. 15, no. 9, pp. 15344–15357, 2014.

[48] P. W. Huisken Mejouyo, O. Harzallah, N. R. S. Tagne et al., "Physical and mechanical characterization of several varieties of oil palm mesocarp fibers using different cross-sectional assumptions," *Journal of Natural Fibers*, vol. 18, no. 2, pp. 175–191, 2021.